An Update on Spatially Variant Apodization and Its Application to Medical Imaging

Jeffrey Arndt and Lauren Kight
KBR

Abstract

Presented here is an extension to the nonlinear apodization (NLA) method known as Spatially Variant Apodization (SVA) for processing magnetic resonance (MR) and ultrasound (US) images. The algorithms presented have modified the original algorithm used in processing radar imagery. This technique also reduces Gibb's artifacts (ringing) while preserving the boundary edges and the mainlobe width of the impulse response. This is done by selecting, pixel-by-pixel, the specific signal-domain windowing function (cosine-on-pedestal) that optimizes each point throughout the image. The windows are chosen from an infinite but bounded set, determined by weighting coefficients for the cosine-on-pedestal equation and the values of the pixels adjacent to the point of interest. By using this method, total sidelobe suppression is achievable without degrading the resolution of the mainlobe. In radar applications, this nonlinear apodization technique has shown to require fewer operations per pixel than other traditional apodization techniques. The preliminary results from applications on MR and US data are presented here as well as an overview of various SVA versions.

Introduction

Recording a continuous band-limited signal with a finite number of samples will always lead to inaccuracies in the reconstruction of the signal due to the lack of available frequency information.

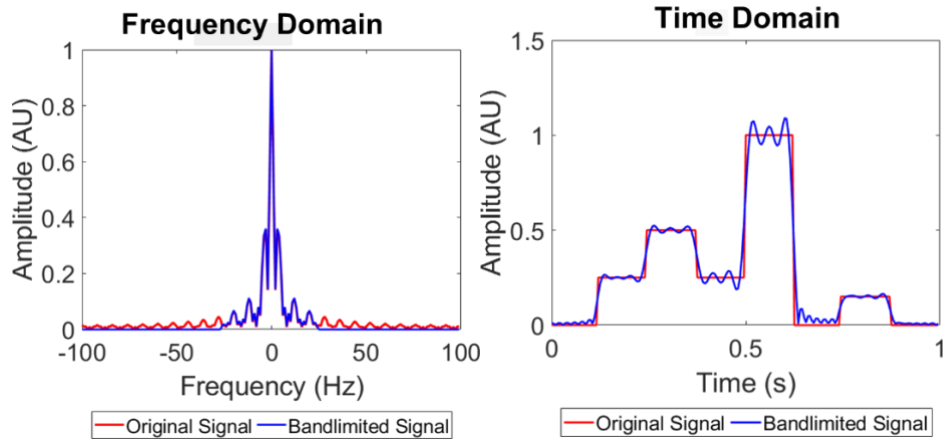

Fig 1. (left) Example of a signal in the frequency domain being bandlimited. Fig 2. (right) The same signals in the time domain. It can be clearly seen how the bandlimited signal has lost information especially near discontinuities/boundaries. This loss of information results in ringing.

Magnetic resonance image acquisition is no exception, as only a finite number of frequencies can be recorded from the current induced in the receiving coils. Hence, the presence of artifacts is unavoidable, specifically Gibb's artifacts (ringing) and blurring. Ultrasound imagery is also limited by sampling factors and the equipment used to reconstruct the image, resulting in similar artifacts. Mitigating these defects is an important component of imaging research and algorithm development. Several highly successful apodization techniques exist in other Fourier imaging domains that have not yet been applied to the medical field. Incidentally, the mathematical similarities in image processing between these different modalities present a unique opportunity for novel applications of image improvement algorithms.

This paper will cover 1D or Classic SVA, Dual SVA, and 5-tap SVA. Classic SVA can be summarized as the weighting of the frequency domain aperture with nonlinear operators that successfully apodizes with no corresponding broadening of the mainlobe [1]. Dual SVA differs from Classic SVA by comparing a generalized non-integer Nyquist sampled SVA version against a "spun" SVA which suppresses diagonal ringing and takes the minimum [2]. Five-tap SVA is a new and efficient technique based on SVA that drastically reduces sidelobe levels

for every sampling rate condition. The algorithm is, essentially, a parameter optimization of a variant filter for each pixel of the image [3].

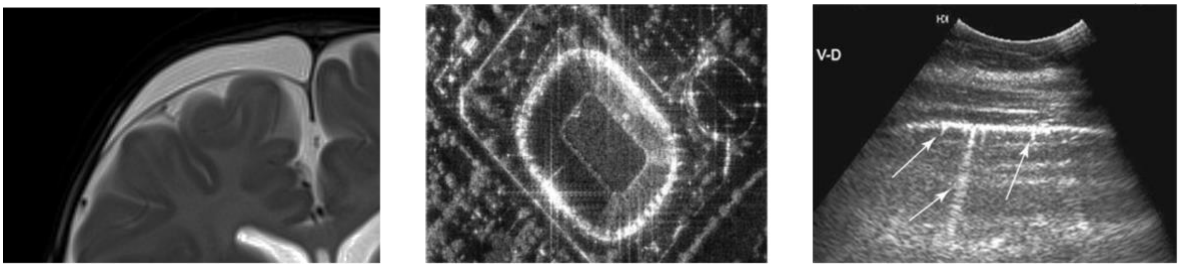

Fig 3. (left) Example of Gibb's artifact (ringing) in the brain near the skull [4]. Fig 4. (middle) Example of ringing in a radar image [3]. Fig 5. (right) Ringing found in an ultrasound image [5].

Classic Nonlinear Apodization (1D SVA)

Apodization refers to the suppression of sidelobes in image processing. Traditional apodization techniques involve the use of windowing functions which can only partially reduce sidelobe levels at the expense of widening the mainlobe and degrading boundary edges. This is especially undesirable when imaging regions that have an increased number of boundaries, such as the brain.

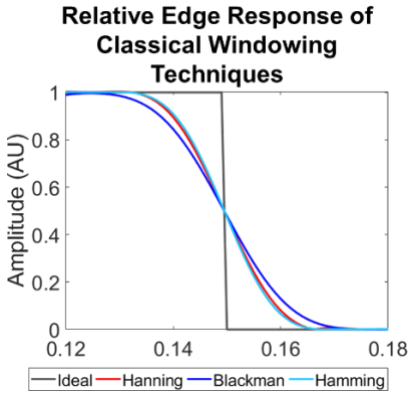

Fig 6. Example of the edge response of classical windowing techniques. This would manifest as blurring in an image due to the lack of sharp transition between values.

SVA is a spatially optimized windowing function formulated around the spatially static cosine windowing function. Each position within the spatial domain corresponds to its own scaled cosine window. This cosine window is optimized over each spatial position to ideally reduce sidelobes while preserving information pertaining to scattering objects. Hence, the window itself is adaptively defined at each image point.

This nonlinear apodization technique was originally developed for improving resolution and reducing ringing in synthetic aperture radar (SAR) imagery [1]. Nonlinear apodization differs from traditional frequency-based processing methods by using an optimization algorithm which uses the values of neighboring pixels to determine the appropriate weighting for the target point. This calculation is repeated for each pixel in the image, producing a new weighting function specifically tailored to yield the optimal value for each point. The result is a computationally efficient suppression of ringing throughout the image.

The most basic version, 1D SVA, will be covered first to provide a foundation for latter versions. The frequency domain cosine-on-a-pedestal weighting function,

$$A(n_i) = 1 + 2w\cos\left(\frac{2\pi n_i}{N}\right) \quad \text{(Eq 1)}$$

with n_i being the index running over the pixel values, w being the weight to be determined, and N being the total length of the array, can be used as a three-point convolver on complex Nyquist sampled images. The weighting

values can range from $w = 0$ (uniform weighting) to $w = 0.43$ (Hamming) to $w = 0.5$ (Hanning). Taking the length-N Fourier Transform of Eq 1 yields the Nyquist-sampled impulse response (IPR)

$$a(m) = w\delta_{m,-1} + \delta_{m,0} + w\delta_{m,+1} \quad \text{(Eq 2)}$$

with m and n being the rows and columns of the pixel and $\delta_{m,n}$ being the Kronecker delta function,

$$\delta_{m,n} = \begin{cases} 1, & m = n \\ 0, & m \neq n \end{cases}. \quad \text{(Eq 3)}$$

A uniformly weighted, complex, Nyquist-sampled image will be denoted as $g(m) = I(m) + iQ(m)$. Using Eq 2 as a three-point convolver on the image $g(m)$ produces

$$g'(m) = w(m)g(m-1) + g(m) + w(m)g(m+1). \quad \text{(Eq 4)}$$

The values for $w(m)$ can range between 0 (uniform weighting) to 0.5 (Hanning weighting). Next, the correct $w(m)$ must be selected to minimize $|g'(m)|^2$ subject to the constraint $0 \leq w(m) \leq 0.5$. The image will be

$$g'(m) = \begin{cases} g(m), & w(m) < 0 \\ 0, & 0 \leq w(m) \leq 0.5 \\ g(m) + 0.5[g(m-1) + g(m+1)], & w(m) > 0.5 \end{cases} \quad \text{(Eq 5)}$$

when the real and imaginary components are solved separately. An overview can be found in the flow chart of Fig 7 and the output and relative edge response of SVA compared to classical windowing techniques in Fig 8 and Fig 9 respectively.

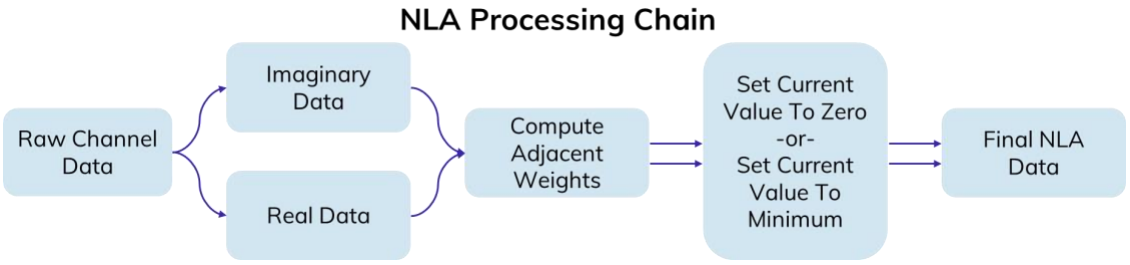

Fig 7. Overview of the processing chain for NLA or SVA. The raw channel data is split into its real (amplitude) and imaginary (phase) components. The adjacent weights are then found and then the output image is found by calculating the ideal weighting function.

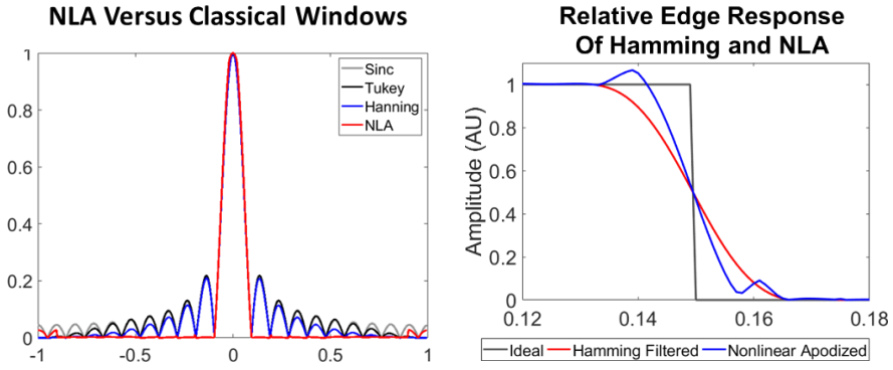

Fig 8. (left) The final output of SVA compared to classical window techniques. SVA completely removes the sidelobes in this case, while the Tukey and Hanning windows only suppress them. Fig 9. (right) The relative edge response of SVA compared to the Hamming window can be seen to be sharper, which results in less blurring of the image.

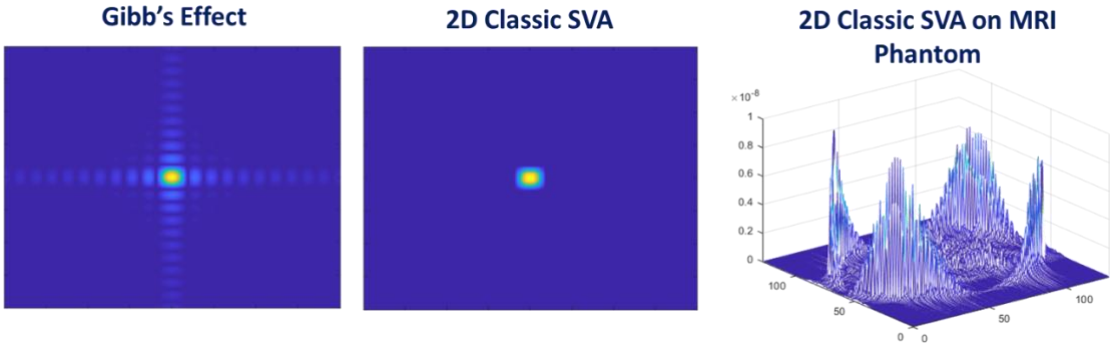

Fig 9. (left) Image with ringing in the cardinal directions. (middle) Output of SVA run horizontally, spinning the image, and then running SVA again. (right) Application of 2D classic SVA on MRI phantom. The ringing has been removed in the cardinal directions, but not in the diagonals.

Dual Spatially Variant Apodization

Dual SVA utilizes a spatially varying window that is optimized for each spatial coordinate in a rectangular grid. Every spatial position on the rectangular grid of the reconstructed image utilizes a scaled form of the selected windowing function. A scaling value is selected such that sidelobes are optimally reduced while maintaining scatterer integrity.

Dual SVA performs two versions of SVA, Generalized SVA (GSVA) and a "spun" SVA, which uses cosine and sine to rotate the kernel to reduce ringing in the diagonal, on the image and selects the output with the minimum absolute value [2]. GSVA is unique from the traditional SVA because it does not require an integer multiple of the Nyquist sampling rate, which is often more practical in actual use [3]. The equation

$$W(f) = a + \sum_{i=1}^{n} 2w_i \cos 2\pi\, f/f_s \qquad \text{(Eq 6)}$$

is used where a is a constraint used to describe the filter based on the image, the sampling frequency is f_s, and f is the frequency with support over the region $-f_0 \le f \le f_0$. The continuum limit impulse response is

$$I(x) = a\, sinc(\pi x) + \sum_{i=1}^{n} w_i \cdot [sinc(2iw_s - 2f_0\pi x) + sinc(2iw_s + 2f_0\pi x)] \qquad \text{(Eq 7)}$$

where w_s is the angular sampling frequency equal to

$$w_s = \pi \frac{f_0}{f_s}. \qquad \text{(Eq 8)}$$

Two constraints are applied which include unit gain, where the weights are restricted to those that pass a direct current signal with unit gain at the origin, and monotonic gain, where only apertures with a gain that monotonically decreases as the magnitude of the frequency increases are considered. The constraint of unit gain is enforced by requiring a to be

$$a = 1 - \sum_{i=1}^{n} w_i \frac{\sin(iw_s)}{iw_s}. \qquad \text{(Eq 9)}$$

If only considering a 3-tap filter, then a becomes

$$a = 1 - w \frac{\sin(w_s)}{w_s} \qquad \text{(Eq 10)}$$

and the weight for the center of the aperture is

$$W(0) = a + w \tag{Eq 11}$$

and the edge is

$$W\left(\frac{f_0}{2}\right) = a + 2w\cos(w_s). \tag{Eq 12}$$

For the monotonicity constraint, w must be within the range

$$0 \le w \le \frac{1}{2\cos(w_s)} \frac{w_s}{\tan(w_s) - w_s}. \tag{Eq 13}$$

The non-integer Nyquist SVA three-point convolver will then become

$$g'(m) = 1 - 2w\frac{\sin(w_s)}{w_s} + w[g(m-1) + g(m+1)]. \tag{Eq 14}$$

The next SVA version used in the DSVA comparison can be found by calculating

$$g''(m) = a'g(m) + w_1'\left[g\left(m - \left\lceil\frac{f_s}{f_0}\right\rceil\right) + g\left(m + \left\lceil\frac{f_s}{f_0}\right\rceil\right)\right] \tag{Eq 15}$$

where

$$a' = 1 - 2w_1' \, sinc\left(\frac{f_0}{f_s}\left\lceil\frac{f_s}{f_0}\right\rceil\right) \tag{Eq 16}$$

and the weights are bound between

$$0 \le w_1' \le \left|\frac{1}{2\left[sinc\left(\frac{f_0}{f_s}\left\lceil\frac{f_s}{f_0}\right\rceil\right) - \cos\left(\pi\frac{f_0}{f_s}\left\lceil\frac{f_s}{f_0}\right\rceil\right)\right]}\right|. \tag{Eq 17}$$

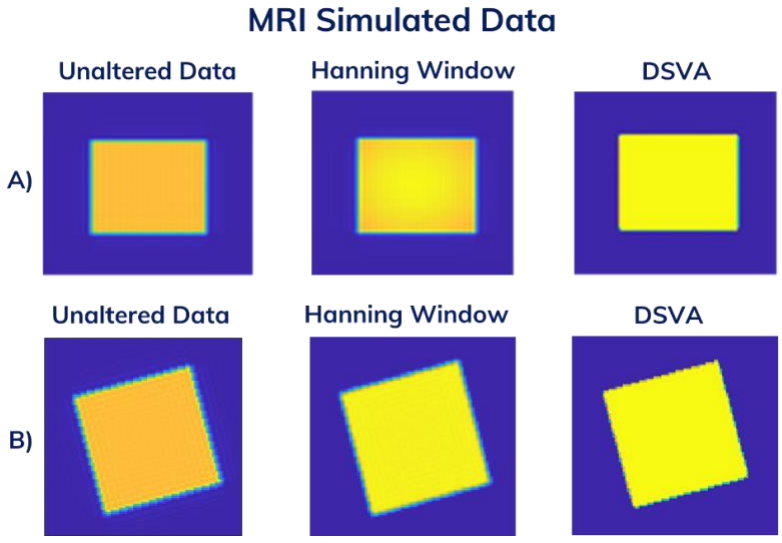

Fig 10. (top left) Unaltered simulated MRI data with ringing. (top middle) Result of Hanning window application. (top right) Output of DSVA on image and ringing has been removed. (bottom left) Unaltered MRI data with ringing in diagonals (bottom middle) Application of Hanning window to noisy image. (bottom right) Output of DSVA on noisy image and the ringing has been removed.

This suppression of ringing and edge blurring in radar imagery allows for improved image interpretability and target recognition. Applications of these nonlinear apodization techniques to medical imagery have the potential to yield images with sharply defined object boundaries, thus allowing for increased precision in identification of anomalies as well as more accurate diagnoses. The "aperture" or receive coils of an MRI machine are not rectangular resulting in ringing in more than just the cardinal directions. This creates a need for ringing reduction in the diagonals as well. It seemed that the application of DSVA would be beneficial; to observe the results DSVA was applied to simulated Magnetic Resonance Images (MRI). Additionally, DSVA was applied to ultrasound (US) data to see if the image quality and interpretability could be improved.

The application of DSVA on simulated MRI data can be found in Fig 10 and Fig 11. The ringing has been removed and there is a marked improvement compared to the Hanning window application.

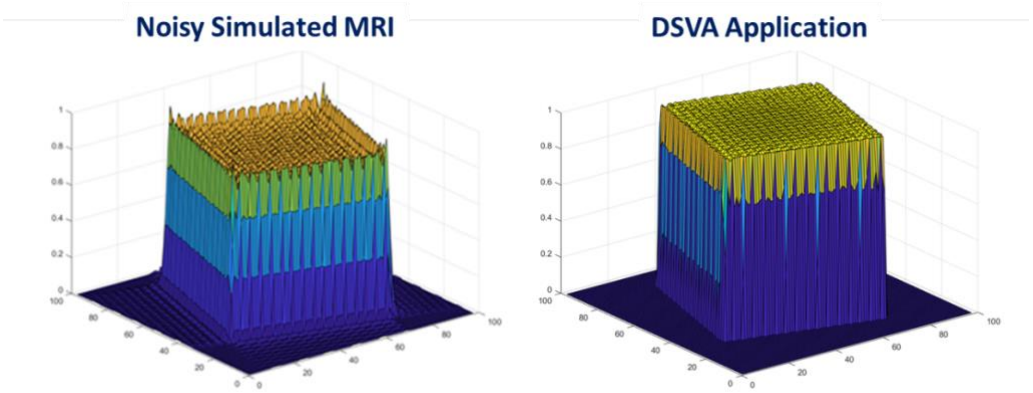

Fig 11. (left) Three-dimensional noisy simulated MRI image. (right) Application of DSVA to noisy simulated MR image which has removed the ringing.

The results of DSVA applied to simulated ultrasound data can be found in Fig 12. There is a significant improvement compared to the Hanning window in both the simulated point targets and the extended target.

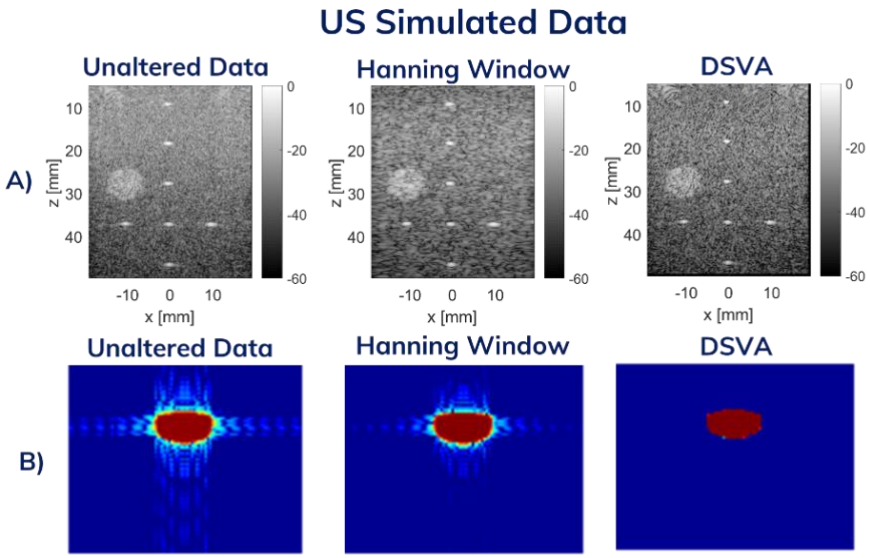

Fig 12. (top left) Unaltered noisy simulated ultrasound data with point targets. (top middle) Application of Hanning window to noisy ultrasound data with some ringing removed. (top right) DSVA applied to noisy data with significant removal of ringing. (bottom left) Unaltered simulated ultrasound data with extended target. (bottom middle) Application of Hanning window with some ringing removed. (bottom right) DSVA applied to noisy image with ringing removed.

Five-Tap Spatially Variant Apodization

This new SVA generalization deals with the other than Nyquist sampling problem, the intent is to preserve the leakage cancellation for any other than Nyquist sampling rate. This will improve Classic SVA through vector optimization.

To increase the removal of ringing in the diagonals, a 5-tap method is explored [3]. In matrix form the continuum limit impulse response will be

$$s(x,y) = I^T(x,y).W(x,y) \tag{Eq 18}$$

$$I^T(x,y) = w_{sx}w_{sy}.\times\begin{bmatrix} sinc(w_{sx}x)sinc(w_{sy}y) \\ \{sinc[w_{sx}(x-1)] + sinc[w_{sx}(x+1)]\}sinc(w_{sy}y) \\ \{sinc[w_{sx}(x-2)] + sinc[w_{sx}(x+2)]\}sinc(w_{sy}y) \\ \{sinc[w_{sy}(y-1)] + sinc[w_{sy}(y+1)]\}sinc(w_{sx}x) \\ \{sinc[w_{sy}(y-2)] + sinc[w_{sy}(y+2)]\}sinc(w_{sx}x) \\ \sum_{\substack{j=\{-1,1\} \\ k=\{-1,1\}}} \{sinc[w_{sx}(x+j)] + sinc[w_{sy}(y+k)]\} \end{bmatrix}$$

$$W(x,y) = \begin{bmatrix} a \\ w_x \\ w_{xx} \\ w_y \\ w_{yy} \\ w_{xy} \end{bmatrix} \tag{Eq 19}$$

With w_{sx} and w_{sy} being the oversampling factor due to zero-padding before the Fourier transform, and the parameter a, which is used to normalize the filter response, is

$$a = 1 - 2w_x sinc(w_{sx}) - 2w_{xx}sinc(2w_{sx}) - 2w_y sinc(w_{sy})$$

$$-2w_{yy}sinc(2w_{sy}) - 4w_{xy}sinc(w_{sx})sinc(w_{sy}). \quad \text{(Eq 20)}$$

The layout of parameter a can be seen in Fig 13.

0	0	w_{xx}	0	0
0	w_{xy}	w_x	w_{xy}	0
w_{yy}	w_y	a	w_y	w_{yy}
0	w_{xy}	w_x	w_{xy}	0
0	0	w_{xx}	0	0

Fig 13. Layout of 5-tap SVA kernel.

The minimization of $s(x, y)$ in Eq 18 is done through optimization of a linear function in 5D hyperspace with constraints,

$$\left.\begin{array}{l} W[k_x, k_x] > 0 \\ \nabla W \cdot \widehat{k_x} < 0 \\ \nabla W \cdot \widehat{k_y} < 0 \end{array}\right| \begin{array}{l} -\frac{N}{2}\Delta k_x \le k_x \le \left(\frac{N}{2} - 1\right).k_x \\ -\frac{M}{2}\Delta k_y \le k_y \le \left(\frac{M}{2} - 1\right).k_y \end{array}. \quad \text{(Eq 21)}$$

Where $\{k_x, k_x\}$ is the principal axis and M and N are the number of samples in the x and y direction. The constraints require that the windows are positive functions whose directional gradients are negative on the principal axis.

The output of the 5-tap SVA application can be found in Fig 14 in both 2D and 3D for easier inspection. Our current code works well with small point targets but needs to be adjusted for application to images.

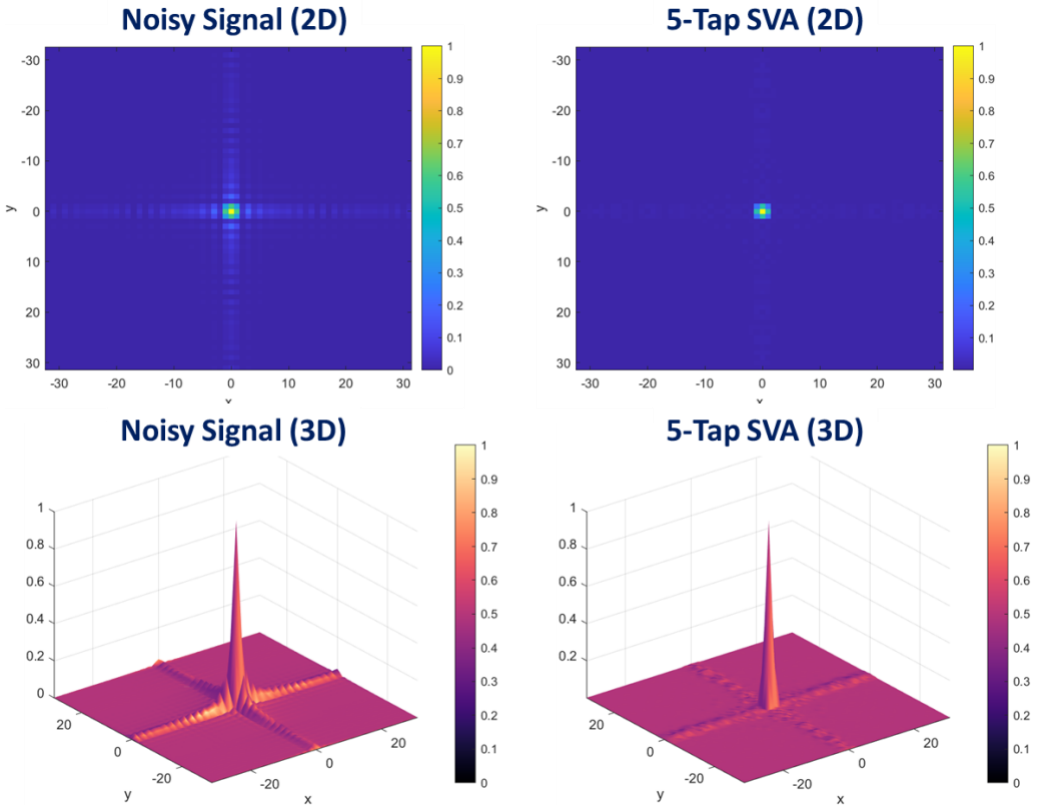

Fig 14. (upper left) Noisy signal in 2D (upper right) 5-tap SVA applied and ringing substantially reduced. (lower left) Noisy signal in 3D (lower right) 5-tap SVA applied and ringing reduced, however, in this image you can see that some sidelobes have not been fully suppressed.

Preliminary Results

The preliminary results for the application of nonlinear apodization techniques on magnetic resonance and ultrasound imagery have shown positive results in suppressing ringing without an increase in blurring or degradation of resolution near the edges in the image. The next steps forward will complete a more detailed statistical analysis of the transferred technique by applying nonlinear apodization to additional simulated and real collected MR and US data.

Acknowledgments

We would like to thank Herbert Stankwitz and Dr. Ron Fairbanks for their assistance in our work. In addition, we are grateful to KBR for continued support in our medical research.

References

[1] H. C. Stankwitz, R. J. Dallaire, J. R. Fienup, “Nonlinear Apodization for Sidelobe Control in SAR Imagery,” IEEE Transactions on Aerospace and Electronic Systems, Vol. 31, No. 1, January 1995.
[2] M. Liu, Z. Li, L. Liu, “A Novel Sidelobe Reduction Algorithm Based on Two-Dimensional Sidelobe Correction Using D-SVA for Squint Images”, Sensors, Vol. 18, No. 3, Mar. 2018.
[3] Smith, B. (2000). Generalization of spatially variant apodization to noninteger Nyquist sampling rates. IEEE Transactions on Image Processing, 9(6), pp.1088-1093.
[4] A. Elster, Gibbs Effect in MR Image of Brain. 2017.
[5] S. Nykamp, "The Equine Thorax", Veterinarian Key, 2016. [Online]. Available: https://veteriankey.com/the-equine-thorax/. [Accessed: 09- Oct- 2019].

Appendix A

Matlab Code for Classic SVA 1D

```
%% Purpose
% This script is performing SVA in one direction on a one dimensional
% image. It must be run on real and imaginary components of the complex
% signal separately.

%% Notes
% The first portion is to wrap around the code as if it were in a circle to
% avoid not performing SVA on the beginning and end of the array. This
% distance will be equal to R, which is the Nyquist rate multiple.

% The second portion is actually performing SVA, which is a nonlinear
% apodization method which selects the optimal cosine-on-pedestal weighting
% function value-by-value throughout the signal. The range is bound between
% [0 0.5], which limits the possibilities and ensure that SVA is
% computationally efficient. It has also been seen in that SVA requires
% relatively less operations per pixel that other nonlinear apodization
% methods.

% Overall this method suppresses sidelobes horizontally along the x-axis.

%% Variables
% g: I or Q data that has already been uniformly weighted
% R: the Nyquist rate multiple (this is pivotal to the code working)
% m: horizontal place in array
% N: length of signal/array
% wrap: how many pixels to wrap around to the end of the array
% behind: the pixel location to be used as the left neighboring pixel for
% weighting
% infront: the pixel location to be used as the right neighboring pixel for
% weighting
% wu: the optimal calculated weight for the cosine-on-pedstal function
% gprime: output signal

%% Code
function [ gprime ] = SVA1D( g, R )

N = length(g);
for m = 1:N
```

```
    % Circular wrapping of location around array
    if m <= R                   % Wrapping around to the back
       m_minusR = N - (R-m);      % spot behind i
       m_plusR = m+R;          % spot in front of i
    elseif m > N-R              % Wrapping around to the front
       m_minusR = m-R;
       m_plusR = (m+R) - N;
    else                        % m can be accessed forwards and backwards
       m_minusR = m-R;
       m_plusR = m+R;
    end

    % Simple 1D SVA code bound between [0 0.5]
    wu = (-g(m))/(g(m_minusR) + g(m_plusR));  % Optimal weight
    % Must be bound between [0 0.5]
    if wu < 0
       gprime(m) = g(m);
    elseif (wu >= 0) && (wu <= 0.5)
       gprime(m) = 0;
    else
       gprime(m) = g(m) + 0.5*(g(m_minusR) + g(m_plusR));
    end


end
```